RSC Applied Polymers

ROYAL SOCIETY OF CHEMISTRY

PAPER

View Article Online
View Journal | View Issue



Cite this: *RSC Appl. Polym.*, 2025, **3**, 137

# Ternary thiol–ene systems as high-performance bone adhesives for potential clinical use†

Lisa Sinawehl, ‡[a,b,d] Patrick Steinbauer,‡[a,b,d] Danijela Kojic,[a,b,d] Paul Slezak,[a,c,d] Heinz Redl[a,c,d] and Stefan Baudis *[a,b,d]

The vision of using bone adhesives for adjunct surgical treatment of complicated fractures or facile reattachment of bone fragments is highly attractive, as compared to conventional techniques, it is expected to significantly reduce operation times and potentially avoid the need for revision surgeries. Nevertheless, no commercial adhesives, that combine biocompatibility, sufficient bonding strength, and time-efficient, implementable fixation protocols are available yet. Inspired by self-etching dental restoratives, we present the development of novel adhesive molecules, so-called primers, containing adhesion motifs for high binding affinity to bone and implants and co-polymerizable groups for incorporation into the adhesive matrix. By efficient design of this primer molecule with regards to spacer length and type and number of polymerizable groups, we were able to develop the first-known one-step *in situ* photocurable adhesive system, based on thiol–ene chemistry with a shear bond strength comparable to dental adhesives. Unprecedented shear bond strength on bone was determined with the optimized system, which surpasses the state-of-the-art thiol–ene adhesive reported in literature by more than 70%. Good *in vitro* biocompatibility of the novel primer was determined, and, remarkably, first *ex vivo* indentation tests on the *calvariae* of rats revealed exceptional adhesive performance with failure of the *calvariae* instead of the adhesive. Due to combining practicability and applicability, this adhesive system might pave the way towards the future of adjunct fracture treatment, with applications such as the fixation of comminuted fractures, small or thin bone fragments, or the additional fixation of implants.

Received 13th March 2024,
Accepted 5th August 2024

DOI: 10.1039/d4lp00094c

rsc.li/rscapplpolym



## Introduction

The number of fracture incidents has been rising steadily due to accidents and a growing number of patients suffering from osteoporosis, with a 33% increase reported since 1990.[1] While simple fractures are treatable with external casts, unstable fractures require surgical intervention and fixation with metallic implants such as plates, screws, and nails.[2–4] Drawbacks associated with these conventional internal fixation procedures, however, include impaired joint mobility due to soft tissue adhesion, a frequent need for secondary intervention, high risk of infections, weak fixation of cancellous bone, and stress shielding caused by the mismatch in modulus between implant and bone.[5–9] Additionally, more complicated traumas, such as comminuted fractures or small bone fragments, are difficult to fix by conventional means. Consequently, osteoporotic fractures often require treatment with more complex procedures such as vertebroplasty, as the reduced bone density may compromise the stability of internal fixation and increase the risk of subsequent fragility fractures.[10] A biocompatible bone adhesive that can be shaped *in situ* and then rapidly cured on demand into a high-strength material could overcome these challenges and provide a quick and easy solution for patient-specific bone repairs.[7] Furthermore, a fast-curing bone adhesive would be a promising alternative to bone cements currently utilized in vertebroplasties. Nevertheless, due to the stringent requirements for these adhesives, no clinically adoptable bone adhesive is commercially available yet, that fulfills the high demands for biocompatibility and adhesive strength while offering a fast and straightforward fixation protocol without multiple application and curing steps.[3,6]

Self-etching dental adhesives are commonly used in dental restorations due to their high adhesive strength, rigidity, and load-bearing properties. Their ease of application, compared to state-of-the-art three-step etch-and-rinse adhesives, makes

[a]*Christian Doppler Laboratory for Advanced Polymers for Biomaterials and 3D Printing, Getreidemarkt 9, 1060 Vienna, Austria*
[b]*Institute of Applied Synthetic Chemistry, TU Wien, Getreidemarkt 9/163 MC, 1060 Vienna, Austria. E-mail: stefan.baudis@tuwien.ac.at*
[c]*LBG Ludwig Boltzmann Institute for Traumatology, The Research Center in Cooperation with AUVA, Donaueschingenstr 13, 1200 Vienna, Austria*
[d]*Austrian Cluster for Tissue Regeneration, 1200 Vienna, Austria*

†Electronic supplementary information (ESI) available. See DOI: https://doi.org/10.1039/d4lp00094c

‡Both authors contributed equally.

them particularly promising for use as surgically feasible bone adhesives.[6,11–14] An essential component in these formulations is adhesive molecules, so-called primers. These primers are comprised of adhesion motifs for binding to dental hard tissue, a spacer that determines specific properties such as volatility, solubility and flexibility, and polymerizable groups for copolymerization with multifunctional monomers that build up the matrix of the dental composite.[13,15] Commonly used (meth)acrylate monomers may exhibit low biocompatibility, and acrylates, in particular, have been observed to cause cytotoxic effects.[16] Additionally, respective polymers exhibit significant shrinkage[17] and may generate acidic degradation products leading to inflammatory responses.[18] Therefore, alternative compounds have been extensively investigated for use as bone adhesives.[19–23] However, biomimetic approaches using fibrin,[24,25] polysaccharides such as chitosan and dextran[26,27] or *O*-phospho-L-serine,[24,28,29] as well as synthetic strategies based on cyanoacrylates[9,30,31] or polyurethanes[32] typically exhibit poor mechanical strength or fail to meet the required standards for biocompatibility.[29,33] Additionally, owing to their different curing mechanisms, these substances do not offer the processability needed during fracture alignment and do not allow bonding on demand through external triggers such as light. In contrast, photocurable thiol–ene chemistry (TEC) employs milder components and achieves high conversions, thereby reducing the leakage of harmful compounds. Due to the stepwise structural buildup, homogeneous and mechanically robust networks are formed, enabling the use of TEC in biomedical applications such as drug delivery vehicles or hydrogels.[34–40] Recently, TEC has been proposed for the development of biocompatible adhesives for fracture fixation.[5–7,41–43] Granskog *et al.* reported an unprecedented shear bond strength of 9.0 MPa using thiol–ene-based primer/matrix systems in combination with a fiber-reinforced adhesive patch (FRAP).[6] Despite these outstanding results, the FRAP methodology is time-consuming due to its multi-step application protocol and therefore must be simplified to be surgically feasible. Recently, Celiz *et al.* developed several one-step photocurable adhesives based on thiol–ene chemistry. While demonstrating good biocompatibility, the low shear bond strength below 1 MPa restricts their use in hard tissue fixation applications.[44]

Herein, we report the first one-step light-curable TEC-based systems containing a vinyl compound, a thiol, and a primer molecule with a previously unprecedented shear bond strength to bone. Inspired by self-etching dental adhesives, we specifically focus on the efficient design of the primer molecule with regard to its spacer length and the type and number of polymerizable groups. The adhesives are characterized regarding cytotoxicity, and bond strength on hydroxyapatite (HAP), titanium, and bovine bone and were applied in *ex vivo* indentation tests. By optimization of the primer structure, surgically feasible one-step adhesives with exceptional shear bond strength can be obtained, paving the way towards facile bone repairs and the potential avoidance of metal implants for fixation of comminuted, low-loaded bone fractures.

# Experimental section

### Reagents and materials

All reagents were purchased from Sigma Aldrich unless otherwise stated. 2,2-Bis(hydroxymethyl)propionic acid (bis-MPA, 98%), allyl bromide (TCI, 98%), *N*,*N*′-carbonyl diimidazole (CDI, abcr, 93%), diethyl(aminomethyl)phosphonate (DAMP, abcr, 97%), trimethylsilyl bromide (TMSBr, 97%), pyridinium *p*-toluenesulfonate (PPTS, TCI, 98%), 6-bromo-1-hexanol (97%), 3,4-dihydro-2*H*-pyran (97%), triethyl phosphite (98%), Amberlite 120 IR, 6-bromohex-1-enyl (TCI, 95%), 4-methoxyphenol (MEHQ, 98%), thioglycerol (TCI, 95%), oxalyl chloride (98%), 5-norbornene-2-carboxylic acid (TCI, 98%), diethyl hydroxymethyl phosphonate (1C-OH, TCI, 97%), sodium hydride (in paraffin oil, TCI, 60%), allyl chloroformate (TCI, 98%), 1,3,5-triallyl-1,3,5-triazine-2,4,6-trione (TAI, TCI, 98%), tris[2-(3-mercaptopropionyloxy)ethyl] isocyanurate TEMPIC (Bruno Bock, 95%) pyrogallol (Merck, 99%), trimethylolpropane tris(3-mercaptopropionate) TMPMP (Bruno Bock, 95%), di-pentaerythritol hexa(3-mercaptopropionate) di-PETMP (TCI, 93%) and molecular sieves (4 Å) were used as received unless otherwise noted. Commercial grade methylene chloride (DCM, Donau Chemie), methanol (MeOH; Donau Chemie), tetrahydrofuran (THF, Donau Chemie), toluene (Donau Chemie) and dioxane (Donau Chemie) were dried with a PureSolvsystem (Inert, Amesbury, MA). Chloroform-*d* ($CDCl_3$, Eurisotop, 99.8%), triethylamine (99.5%), and pyridine (99.8%) were dried over 4 Å molecular sieves. The photoinitiator bis(4-methoxybenzoyl) diethylgermanium (Ivocerin®) was kindly provided by Ivoclar Vivadent AG and used as received.

### Primer synthesis

The detailed syntheses and characterization of all primer molecules are given in the ESI chapter 1.†

### Functionalization step

**General procedure A.** The functionalization of the respective building blocks (1C-OH, 6C-OH, or 6C-diOH) with norbornene groups was conducted in accordance with a general esterification procedure of acid chlorides with alcohols.[45] Freshly prepared norbornene chloride (NB-Cl) was added dropwise to a mixture of the respective building block and TEA in dry methylene chloride (DCM) at 0 °C under argon atmosphere. The solution was stirred for 1 h at 0 °C and 24 h at room temperature (RT), after which the solvent and residual starting material were removed *in vacuo*. The obtained crude product was dissolved in 50 mL DCM, and subsequently, the solution was washed with brine (3 × 25 mL). The combined organic layers were dried over $MgSO_4$, and the solvent was evaporated. The obtained product was either used without further purification or purified *via* silica flash column chromatography, if necessary.

**General procedure B.** The Williamson ether synthesis to functionalize the building blocks with allyl ether groups was conducted according to Sasaki *et al.*[46] Sodium hydride in

paraffin oil was suspended in dry THF under argon atmosphere. The respective building block was diluted in 10 mL THF and added slowly *via* syringe at 0 °C. After 1 h, allyl bromide was added *via* syringe. Then, the ice bath was removed, and the reaction mixture was stirred at RT overnight. After removal of the solvent and residual starting materials *in vacuo*, the crude product was purified *via* silica flash column chromatography.

**General procedure C.** The functionalization with allyl carbonate groups was conducted similarly to a procedure by Trost *et al.*[47] The respective building block and dry pyridine were dissolved in DCM under argon atmosphere. Allyl chloroformate was added dropwise *via* syringe at 0 °C. After stirring for 1 h at 0 °C, the ice bath was removed, and the reaction was stirred at RT overnight. The crude product was dissolved in dry ethyl acetate to precipitate the pyridinium salts, which were filtered off. The solvent was evaporated, and the obtained product was either used without further purification or purified *via* silica flash column chromatography, if necessary.

### Deprotection step

**General procedure D.** The dealkylation of the functionalized intermediates was performed similarly to Chougrani *et al.*[48] Trimethylsilyl bromide (TMSBr) was added to a solution of the intermediate in dry DCM. The reaction mixture was stirred for 20 h at 30 °C and then concentrated under reduced pressure. 50 mL of methanol were added, and the solution was stirred at RT for 5 h. After evaporation of the solvent, the product was used without further purification.

### Preparation of formulations

All formulations were prepared in an orange light laboratory with wavelengths below 480 nm filtered out to avoid light exposure. All polymerizations were carried out in bulk, without solvent by photopolymerization. As a radical photoinitiator (PI), Ivocerin® (bis-(4-methoxybenzoyl)diethylgermanium) was used. 0.02 wt% of pyrogallol were added for stabilization.

### Two-step formulation

For the two-step procedure, a matrix and a primer formulation were prepared. The primer formulation consisted of the vinyl compound TAI (12.5 wt%) and the thiol TEMPIC (71 wt%), to which an additional 15 wt% of the respective primer was added, resulting in a thiol : ene ratio of roughly 2 : 1 in this formulation. Furthermore, the primer formulation contained 1.5 wt% Ivocerin and 0.02 wt% pyrogallol.

The matrix formulation consisted of the vinyl compound TAI (32 wt%) and the thiol TEMPIC (67 wt%) in a molar ratio of vinyl to thiol groups of 1 : 1, as well as 1 wt% of the photoinitiator and the 0.02 wt% stabilizer.

### One-step formulation

For the one-step procedure, only the aforementioned primer formulation containing primer (15 wt%), vinyl compound TAI (27 wt%), thiol TEMPIC (57 wt%), photoinitiator (1 wt%), and stabilizer (0.02 wt%) was prepared.

### Characterizations

**NMR spectra.** NMR spectra were recorded at room temperature on a Bruker Avance at 400 MHz for $^{1}$H, 101 MHz for $^{13}$C, and 162 MHz for $^{31}$P-NMRs. The samples were dissolved in $CDCl_3$ and referenced to the solvent residual peak. Chemical shifts are given in ppm, multiplicities are termed s (singlet), d (doublet), t (triplet), q (quartet), and m (multiplet), and coupling constants ($J$ values) are given in hertz. The data was processed with the software TopSpin 3.5 pl 7 from Bruker.

**Shear bond strength (SBS)-measurements.** The detailed setup, measurement procedure, and preparation of the substrates for the shear-bond strength measurements can be found in the ESI.†

For the execution of the two-step procedure, the primer formulation was rubbed on the substrate surface with a dental microbrush for 20 s. After an air-drying phase of 5 s at room temperature, the formulation was cured for 10 s with a Bluephase C8 dental lamp (385–515 nm, 720 mW cm$^{-2}$). A polypropylene (PP) mold insert was placed on the top of the substrate surface and fixated with a clamping tool, whereafter, the matrix formulation was applied into the mold cavity and cured for 20 s.

For the one-step procedure, the primer formulation was pipetted into the PP mold cavity and subsequently light-cured for 20 s. The samples were stored in modified simulated body fluid, m-SBF (prepared according to Oyane *et al.*[49] at 37 °C for 24 h) before the measurements. The SBS was determined by shearing off the obtained adhesive pins with a digital force measuring device (Force Gauge SF-30) with a V-shaped bar. Five samples of every formulation and substrate were tested.

***Ex vivo* indentation tests.** *Ex vivo* experiments were conducted on dead rat specimen at LBG Ludwig Boltzmann Institute for Traumatology. All animals were euthanized as part of other experiments not related to this study. All nessecary permits and ethical approval were obtained by the institute and no additional ethical statement was needed for experiments conducted on cadavers. *Ex vivo* Indentation Tests were performed in circular bone defects with a diameter of 8 mm that were excised centrically from the calvariae of 4 dead male Sprague Dawley rats with a weight of approximately 500 g, (Janvier-Labs, France) using a hole saw. In two rats, the excised calvariae plates were re-fixated in the cranium using the bone adhesive at the edge of the defect. In the other two rats, the adhesive was applied to cover the entire *calvariae* after repositioning of the excised plate defect and was subsequently cured with a Bluephase C8 dental lamp for 20 s. Indentation tests were then performed with a digital force measuring device (Force Gauge SF-30 with a conical tip) to determine the stability of the calvaria.

**Evaluation of cytotoxicity.** *In vitro* cytotoxicity of the vinyl compound TAI, the thiol TEMPIC, and the primer 6C-diNB was tested in NCTC Clone 929 fibroblast cell culture using a Presto® Blue Assay according to ISO-10993-5. The cells were cultured in Dulbecco's modified Eagle's medium (DMEM) supplemented with 10% fetal bovine serum (FBS) and penicillin–streptomycin (Pen-Strep) (100 U mL$^{-1}$ penicillin and 100 μg

$mL^{-1}$ streptomycin), in 96-well plates at a density of 1 $10^4$ cells per well for 24 h in humidified air with 95% relative humidity and with 5% $CO_2$ at 37 °C. All compounds were dissolved in DMSO to obtain 1 M solutions, which were then further diluted with DMEM, 10% FBS, 100 U $mL^{-1}$ penicillin and 100 μg $mL^{-1}$ streptomycin, to obtain solutions with the concentrations 0.01 mol $L^{-1}$, 0.0075 mol $L^{-1}$, 0.005 mol $L^{-1}$, and 0.0025 mol $L^{-1}$. After 24 h, the cells were treated with 100 μL of each solution in triplicates and incubated at 37 °C for 24 h. Qualitative screening of morphological changes was conducted microscopically according to ISO 10993-5. For quantitative screening of cell viability, the supernatant solution was removed, and 10 μL of resazurin were added to the cells. After 1 h at 37 °C, the fluorescence intensity was measured at 570 nm. As control values, cells treated with 1% DMSO solution, a blank value, and PBS buffer were used. The results represent the mean of triplicate measurements. The background fluorescence was subtracted from each measurement signal and the viability of the negative control was assumed to be 100%. The viability of the treated cells was calculated by dividing the mean of the treated cells by the mean of the control culture on the respective cell culture plate. The concentration at which 80% of the cells are still viable after 1 d was used to determine the cytotoxic limit.

# Results and discussion

## Design of self-etching primers

Inspired by dental adhesives, we chose a two-component system comprised of the rigid trifunctional thiol tris[2-(3-mercaptopropionyloxy)ethyl] isocyanurate (TEMPIC) and the vinyl compound triallyl isocyanurate (TAI) as the basis for the adhesive formulation (Fig. 1A). Given that the high *in situ* bonding strength of dental restoratives can be mainly attributed to the self-etching primer present in the formulation, we focused on designing novel primer molecules.

Based on recent studies revealing high adhesion of the phosphoprotein statherin to hydroxyapatite, the phosphonic acid group was chosen as an adhesion motif.[50] This motif enables adhesion to bony substrates by dissolving HAP, exposing collagen fibers for entanglement surface binding, and forming both ionic and covalent bonds with the hard tissue surface.[6,7,11,50] To develop a formulation curable in fewer steps than state-of-the-art systems while providing adequate bonding strength, we hypothesized that the primer molecule should contain a polymerizable group, with a different reactivity towards thiol–ene polymerization compared to the ene-functionality of the monomer. This difference in reactivity would enable full incorporation of the primer into the matrix

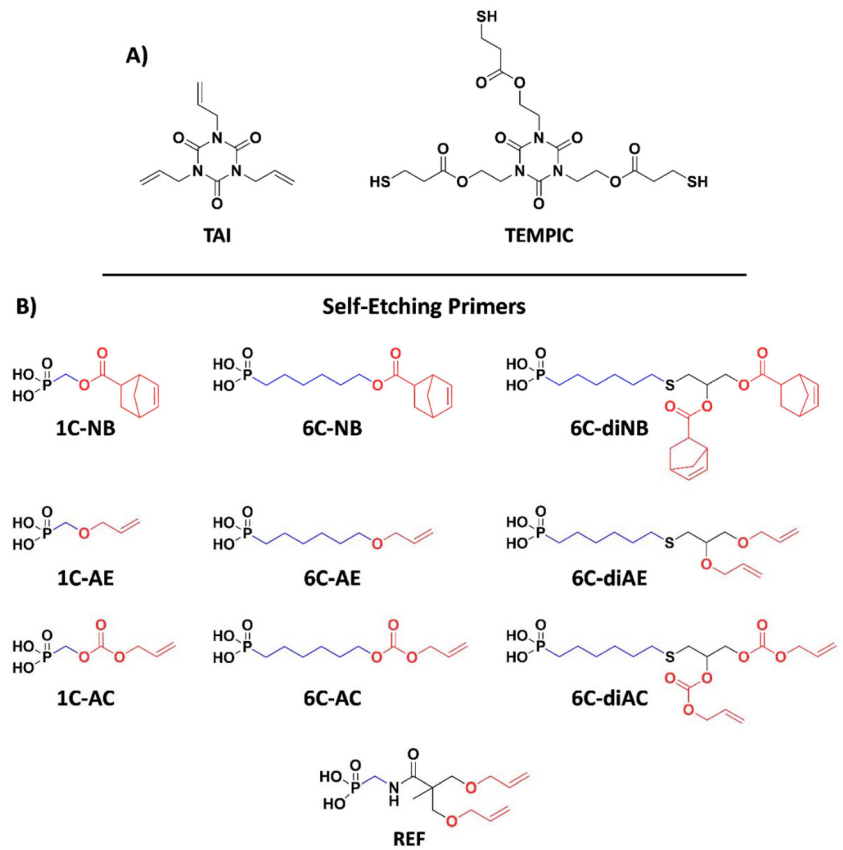


**Fig. 1** Schematic representation of the compounds of the TEC-adhesive formulation: (A) thiol–ene matrix consisting of TAI and TEMPIC and (B) structures of the novel primer molecules containing different spacer lengths (1C or 6C, marked in blue) and type and number of polymerizable groups ((di)NB, (di)AE, (di)AC, marked in red) as well as the difunctional allyl ether reference primer (REF) used by Granskog *et al.*[6]

network and enhance its anchoring on the bone surface. Norbornenes, allyl ethers, and allyl carbonates were selected as polymerizable groups due to their higher reactivity towards TEC compared to the unhindered ene moiety in TAI, as previously shown by Hoyle and Bowman *et al.*,[39,40,51] as well as in our recent study.[52] We further assumed that the number of polymerizable groups and the spacer length would impact the resulting adhesive strength as well. As a result, a series of primer molecules was synthesized starting from building blocks with different spacer lengths (1C-OH, 6C-OH, or 6C-diOH) and a protected phosphonic adhesion motif (Fig. 1B). The initial reaction step involved the functionalization with different polymerizable groups (norbornene = NB, allyl ether = AE or allyl carbonate = AC, Scheme S1 I†). Norbornene and allyl carbonate functionalities were introduced *via* esterification with the corresponding acid chlorides according to Carlise *et al.*[45] and Trost *et al.*,[47] respectively, while allyl ethers were synthesized using Williamson ether synthesis according to Sasaki *et al.*[46] To obtain the final primer structure, a hydrolysis step was performed to deprotect the phosphonic acid (Scheme S1 II†). As a reference, the difunctional allyl-ether primer (**REF**, Fig. 1B) used in photopolymerizable TEC systems by Granskog *et al.*[6] was synthesized. All novel primers were obtained in good yields, and 20 wt% solutions in ethanol/water (1 : 1 w/w) exhibited pH values below 2, confirming their sufficient acidity for self-etching properties comparable to commercial dental primers (Table S1†).[53]

## Bonding strength

To assess the bond strength of the adhesive systems containing different primer molecules, shear bond strength measurements were performed. These measurements are particularly reliable for determining the adhesive strength of stiff materials requiring high shear rates, making them a standard method for evaluating the adhesive properties of dental materials.[13,54] Thereby, a resin pin is polymerized onto a substrate surface and sheared off parallel to the bonded surface (Fig. 3D).[55] As a substrate, hydroxyapatite (HAP) with a defined surface roughness was used to mimic the mineral phase of bone. Additionally, tests were performed on $TiO_2$ to determine the bond strength to the surface of implants, with the detailed results given in the ESI (Tables S5 and S6†). The setup and the preparation of all substrates are shown in the ESI (Fig. S1 and S2†).

In general, two different workflows were used for applying the adhesive, which are depicted in Fig. 2. In the two-step procedure, a thin layer of primer formulation containing the synthesized primer molecule, vinyl compound, thiol, initiator, and stabilizer was applied and then cured within seconds with a dental UV lamp (385–515 nm, 720 mW $cm^{-2}$). To polymerize the resin pin onto this pre-treated surface, a mold was clamped onto the substrate, and the matrix formulation containing the vinyl compound, thiol, and the initiator was applied and subsequently cured.

In the one-step procedure, the primer formulation was directly applied to the mold without prior surface treatment and cured with the dental lamp. This approach is far more practical and time-efficient for surgical applications. To mimic physiological conditions, all samples were immersed in modified simulated body fluid at 37 °C for 24 h before evaluating the shear bond strength.

To ensure high curing depths and efficient polymerization, the biocompatible photoinitiator Ivocerin, which is also used in dental restoratives, was selected due to its red-shifted maximum absorption wavelength of 408 nm.[56] For optimal mechanical performance, precise control of the stochiometric ratio between thiol and ene groups is essential for a proper progression of the polymerization. In the matrix formulation, a molar ratio of 1 : 1 of vinyl and thiol groups was used. Preliminary studies for the primer formulation indicated that a slightly off-stoichiometric ratio of thiol to total vinyl groups (2.2 : 1 thiol : ene, TAI, and primer molecule) results in residual thiol groups, which then enhance covalent binding of the matrix to the primer network and lead to higher SBS (Fig. S3 and Table S2†). Additionally, various thiols were evaluated, and it was found that the highest SBS was achieved with TEMPIC (Fig. S4 and Table S3†).

Next, it was shown that precise control over the primer content in the formulation is crucial. Phosphonic acid moieties, which are present in the primer molecules, are commonly used as stabilizers in TEC formulations due to their ability to trap radicals and thereby may impede the polymerization process. Our findings revealed that the highest shear

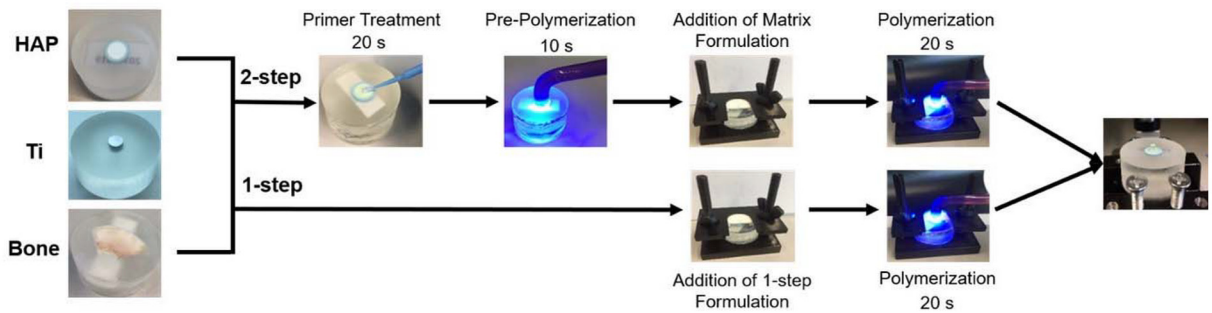


Fig. 2 Workflows for application of the TEC adhesive for SBS measurements to the different substrates. Two-step procedure with the pre-treatment with the primer formulation, pre-polymerization, the addition of matrix formulation followed by the final polymerization step. One-step procedure with the addition of the primer formulation followed by the final polymerization step.

bond strength was achieved with a primer concentration of 15 wt% (Fig. S5 and Table S4†). This concentration corresponds to a molar ratio of phosphonic groups relative to the TEC functional groups ranging from 0.04–0.12 for all formulations. This ratio, also reported by Granskog *et al.*,[6] is presumed optimal as it ensures that all phosphonic acid groups are bound to the substrate surface without excess groups that could interfere with the radical polymerization.

A comprehensive investigation further revealed the effects of spacer length, as well as the type and number of polymerizable groups on SBS for both the two-step and the one-step system (Fig. 3A–C and Tables S5, S6†).

For both procedures, increasing the spacer length from one carbon to six carbons resulted in higher SBS. This improvement may be attributed to the increased flexibility in the primer structure, which enhances its orientation on the substrate surface and thereby increases bond strength. Another explanation might be that upon contact of the primer with the substrate surface, an insoluble salt is formed between the phosphoric acid moiety and the calcium ions. As primers with six carbon atom spacers create a more hydrophobic environment, the equilibrium shifts more towards the insoluble salt, producing a stronger bond compared to less hydrophobic primers with one carbon spacers. Additionally, primer molecules bearing norbornene groups demonstrated higher SBS compared to allyl ethers and allyl carbonates. This is due to the significantly increased reactivity of norbornene groups towards thiol–ene polymerization, as confirmed by previous studies (Fig. 3A and B).[52] Thereby, the consumption of norbornene moieties is prioritized, ensuring that most primer molecules are covalently connected to the thiol–ene matrix.

For all two-step systems, a further improvement of SBS was observed by increasing the number of polymerizable groups from one to two. An explanation is that additional polymerizable groups provide more binding sites for the TEC matrix, which further enhances the incorporation of the primer into the matrix network and reduces the potential for adhesive failure. Again, this effect was most pronounced with norbornene-bearing primer molecules (Fig. 3A).

In the one-step procedure, SBS measurements could not be performed with 1C-NB due to strong discoloration of the formulation, which hindered light penetration and polymeriz-

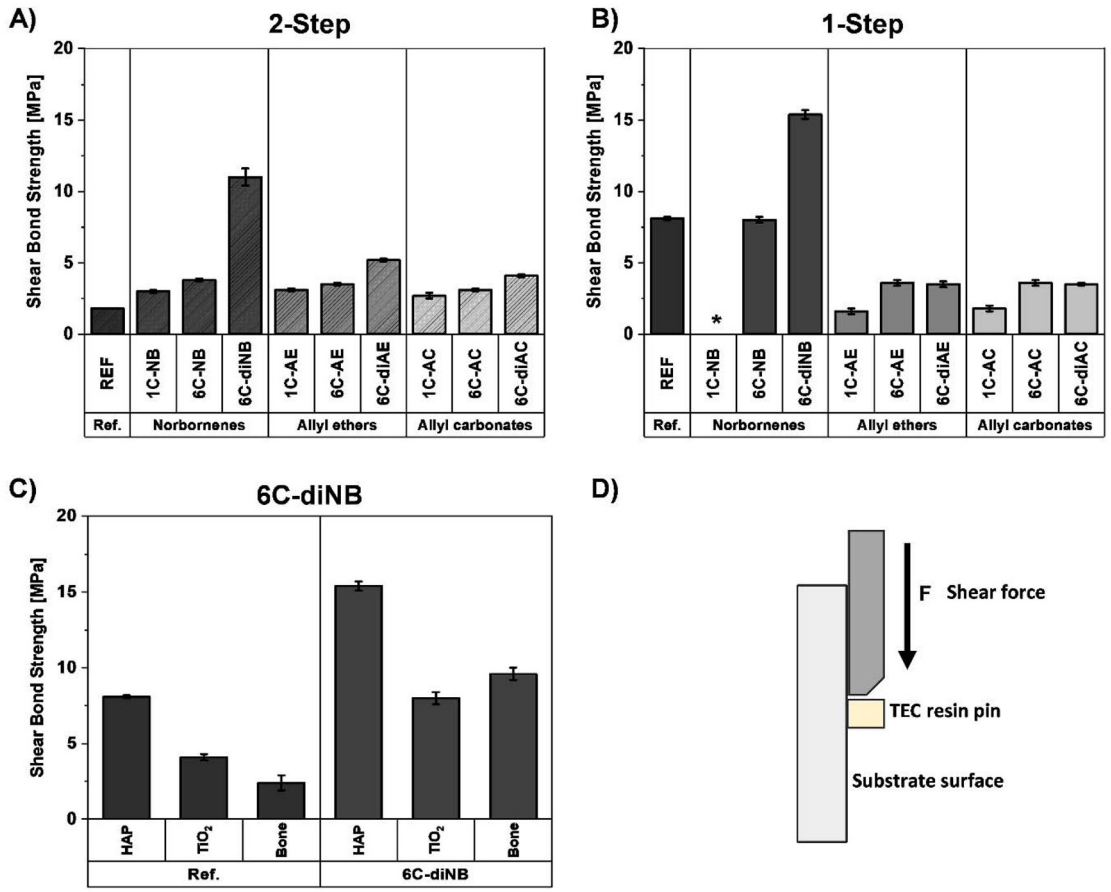


**Fig. 3** Results of SBS measurements of the (A) two-step and (B) one-step adhesive systems containing 15 wt% Primers, 27 wt% TAI, 57 wt% TEMPIC, and 1 wt% Ivocerin®, ranked according to the spacer length as well as the type and the number of polymerizable groups. (C) Comparison of the one-step systems containing either the reference primer or 6C-diNB on the different substrate surfaces HAP, titanium, or bovine bone; (D) schematic representation of the SBS-measurement procedure. *Due to strong discoloration of the formulation, only partial curing and as a result no testing was possible.

ation. For the other systems with a one-carbon spacer (1C-AE and 1C-AC) no significant differences in SBS were determined. Although increasing the spacer length enhanced the SBS, an increase in the number of allyl ether or allyl carbonate groups, did not improve the SBS of the one-step system. In contrast, primers containing norbornene groups exhibited the highest SBS, with a significant further increase when two polymerizable groups were used. This underscores the importance of two highly reactive groups within the primer structure (Fig. 3B) to ensure complete incorporation into the polymer matrix. An unprecedented SBS of 15.4 MPa (±0.3 MPa) was obtained with 6C-diNB, significantly surpassing the reference system despite its lower molar proportion due to increased molecular weight. Remarkably, this SBS even exceeded the values reported for commercial dental adhesive systems, such as Clearfil SE Bond, with a SBS of 5.8 MPa (±0.1 MPa),[6] and outperforms the multi-step FRAP methodology using TEC-adhesives by 71%.[6] The high surface bonding strength of this one-step system was also confirmed on titanium and in *ex vivo* measurements on bovine bone (Fig. 3C). As a control experiment and to mimic the conditions present during surgical procedures, measurements were also performed on wetted bone surfaces. Results showed that when a short air-drying step of 5 s was applied, no discernable differences in SBS were observed. (Table S7 and Fig. S6†). Additionally, to incorporate degradable moieties into the material, in recent studies the ene monomer TAI was partially replaced by the hydrolytically cleavable boronic ester monomer 1,4-bis(4-vinyl-1,3,2-dioxaborolan-2-yl)benzene (vinyl dioxaborolane, VDB, Fig. S7 A†). SBS results indicated that bond cleavage occurred during storage in modified-simulated body fluid resulting in a softened network with reduced SBS (Table S8 and Fig. S7B†). Since this degradation is proceeding fast, future studies will be conducted to further tune the degradation profile of the employed matrix monomers.

### *Ex vivo* indentation tests

As an initial proof of concept, *ex vivo* tests were performed on the most promising one-step system containing the primer 6C-diNB (Fig. 4). The *calvariae* of 4 rats were removed using a hole saw, and the excised bone plates were reattached to the cranium with the adhesive. For two test specimens, the adhesive was applied only on the edges of the plate and cured for reattachment. For the remaining rats, the formulation was applied over the entire bone plate and cranium-calvaria edges before polymerization. The stability of the treated defect was assessed *via* indentation tests using a conical tip (Fig. S8†). For all specimens unprecedented indentation forces were shown (Table S9†) with failure occurring in the calvariae rather than in the adhesive, further corroborating its superior adhesive performance.

### Cytotoxicity

Photopolymers used *in vivo* may cause leakage of residual unreacted compounds into surrounding tissues. To estimate the concentration of these residual compounds after polymerization, photorheology[57] studies were performed. These studies revealed a high efficiency of the thiol–ene polymerization, with double bond conversions exceeding 70% for the one-step formulation (Fig. S10 and Table S11†). According to this and assuming equal consumption of the double bonds and thiol groups, all compounds should be incorporated into the polymer network with at least one functionality. Nevertheless, to ensure that potentially unreacted substances do not cause any adverse effects, cell viability tests were conducted using a Presto® Blue Assay with mouse cells (NCTC Clone 929). The cells were incubated for 24 h with varying concentrations of the vinyl compound TAI, the thiol TEMPIC, and the most promising primer 6C-diNB. Concentrations ranged from 2.5 to 10 mmol $L^{-1}$. In addition to this quantitative screening, a qualitative microscopic assessment revealed no morphological changes in the cells caused by the substances (Figure S9†). The concentration at which 80% of the cells remained viable after the incubation time (effective concentration, $EC_{80}$) was used to evaluate the cytotoxic limit of the compounds (Table 1 and Table S10†).

High $EC_{80}$ values were determined for both the monomer TAI and the novel primer molecule. Accordingly, these compounds demonstrated high tolerance by the cells and exerted sufficiently low toxic effects on the fibroblast cells. This highlights the benign nature of the novel high-performance primer. Although no morphological changes were observed in the cells treated with solutions of the thiol TEMPIC (Fig. S9B†), quantitative screening revealed a slight cytotoxic potential for this compound with viabilities of 46% at 2.5 mM. Nonetheless, due to the high conversions of the compounds determined in photorheology measurements, the possibility of

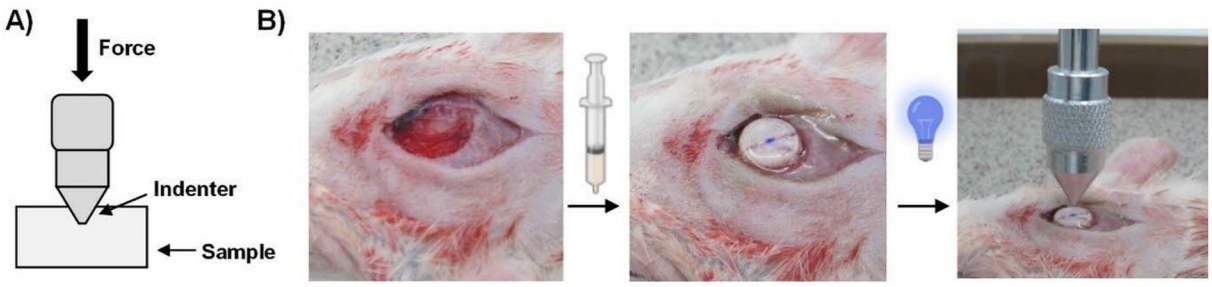


Fig. 4 (A) Schematic overview of the indentation test, (B) *ex vivo* indentation test of the fixated rat *calvariae*.

Table 1 Cytotoxic effect ($EC_{80}$ values) of the vinyl compound TAI, the thiol TEMPIC, and the primer 6C-diNB

| Substance | $EC_{80}$ (mM) |
|---|---|
| **TAI** | 5.0 |
| **TEMPIC** | <2.5 |
| **6C-diNB** | 5.0 |

the presence of unreacted compounds is neglectable. Thus, the concentrations of potentially unreacted components are expected to be sufficiently low, though this still needs to be confirmed through upcoming *in vivo* tests.

## Conclusion

Despite three decades of research, no surgically adoptable bone adhesive has been identified that combines biocompatibility, sufficient bonding strength, and ease of application. Inspired by self-etching dental adhesives, we developed novel primer molecules for use in a ternary thiol–ene adhesive formulation, by varying spacer length, type, and number of polymerizable groups. By increasing the spacer length and incorporating two ene moieties with higher reactivity towards the thiol component compared to the vinyl compound, improved primer incorporation into the matrix network was achieved. Most remarkably, these novel adhesives could be applied in a time-efficient, surgically preferred one-step process without the need of additional fiber reinforcement to achieve sufficient mechanical strength. Unprecedented high SBS on hydroxyapatite, bone, and titanium was obtained with the system containing the novel primer 6C-diNB. Impressively, this system by far exceeded state-of-the-art bone adhesives and even outperformed commercial dental adhesives. Finally, *ex vivo* tests proved the excellent adhesive performance while good biocompatibility of the novel primer was shown *in vitro*. This demonstrates the great potential of this one-step system as a high-performance bone adhesive, which can be shaped *in situ* and then rapidly cured by UV light and potentially used for the fixation of comminuted fractures, and small or thin bone fragments. This system combines practicability and applicability and may therefore serve as a support for fracture treatment in the future. Further work will focus on determining long-term local tissue responses and *in vivo* toxicity of this novel adhesive in animal models.

## Data availability

The data supporting this article have been included as part of the ESI.†

## Conflicts of interest

There are no conflicts to declare.

## Acknowledgements

Funding by the Christian Doppler Research Association within the framework of the "Christian Doppler Laboratory for Advanced Polymers for Biomaterials and 3D Printing" and financial support by the Austrian Federal Ministry for Digital and Economic Affairs and the National Foundation for Research, Technology, and Development are gratefully acknowledged. The authors acknowledge TU Wien Bibliothek for financial support through its Open Access Funding Program.

## References

1 A.-M. E. A. Wu, *Lancet Healthy Longev*, 2021, **2**, e580–e592.
2 M. J. Sánchez-Fernández, H. Hammoudeh, R. P. Félix Lanao, M. van Erk, J. C. M. van Hest and S. C. G. Leeuwenburgh, *Adv. Mater. Interfaces*, 2019, **6**, 1802021.
3 K. O. Böker, K. Richter, K. Jäckle, S. Taheri, I. Grunwald, K. Borcherding, J. von Byern, A. Hartwig, B. Wildemann, A. F. Schilling and W. Lehmann, *Materials*, 2019, **12**, 3975.
4 C. Heiss, R. Kraus, D. Schluckebier, A.-C. Stiller, S. Wenisch and R. Schnettler, *Eur. J. Trauma*, 2006, **32**, 141–148.
5 M. Arseneault, V. Granskog, S. Khosravi, I. M. Heckler, P. Mesa-Antunez, D. Hult, Y. Zhang and M. Malkoch, *Adv. Mater.*, 2018, **30**, 1804966.
6 V. Granskog, S. García-Gallego, J. von Kieseritzky, J. Rosendahl, P. Stenlund, Y. Zhang, S. Petronis, B. Lyvén, M. Arner, J. Håkansson and M. Malkoch, *Adv. Funct. Mater.*, 2018, **28**, 1800372.
7 D. J. Hutchinson, V. Granskog, J. von Kieseritzky, H. Alfort, P. Stenlund, Y. Zhang, M. Arner, J. Håkansson and M. Malkoch, *Adv. Funct. Mater.*, 2021, **31**, 2170302.
8 K. O. Böker, K. Richter, K. Jäckle, S. Taheri, I. Grunwald, K. Borcherding, J. von Byern, A. Hartwig, B. Wildemann, A. F. Schilling and W. Lehmann, *Materials*, 2019, **12**, 3975.
9 D. F. Farrar, *Int. J. Adhes. Adhes.*, 2012, **33**, 89–97.
10 X. Author, *Orthop. Surg.*, 2009, **1**, 251–257.
11 Y. Catel, S. Schörpf and N. Moszner, *Macromol. Mater.*, 2015, **300**, 1010–1022.
12 N. Moszner and T. Hirt, *J. Polym. Sci., Part A: Polym. Chem.*, 2012, **50**, 4369–4402.
13 N. Moszner, U. Salz and J. Zimmermann, *Dent. Mater.*, 2005, **21**, 895–910.
14 J. L. Ferracane, *Dent. Mater.*, 2011, **27**, 29–38.
15 D. H. Pashley, H. Sano, B. Ciucchi, M. Yoshiyama and R. M. Carvalho, *Dent. Mater.*, 1995, **11**, 117–125.
16 C. Heller, M. Schwentenwein, G. Russmueller, F. Varga, J. Stampfl and R. Liska, *J. Polym. Sci., Part A: Polym. Chem.*, 2009, **47**, 6941–6954.
17 H. B. Bingol, J. C. M. E. Bender, J. A. Opsteen and S. C. G. Leeuwenburgh, *Mater. Today Bio*, 2023, **19**, 100599.
18 S. Orman, C. Hofstetter, A. Aksu, F. Reinauer, R. Liska and S. Baudis, *J. Polym. Sci., Part A: Polym. Chem.*, 2019, **57**, 110–119.

19 S. Orman, C. Hofstetter, A. Aksu, F. Reinauer, R. Liska and S. Baudis, *J. Polym. Sci., Part A: Polym. Chem.*, 2018, **57**, 110–119.
20 B. Husár, C. Heller, M. Schwentenwein, A. Mautner, F. Varga, T. Koch, J. Stampfl and R. Liska, *J. Polym. Sci., Part A: Polym. Chem.*, 2011, **49**, 4927–4934.
21 N. L. Davison, F. Barrère-de Groot and D. W. Grijpma, in *Tissue Engineering*, 2014, pp. 177–215, DOI: 10.1016/b978-0-12-420145-3.00006-7.
22 A. Mautner, B. Steinbauer, S. Orman, G. Russmüller, K. Macfelda, T. Koch, J. Stampfl and R. Liska, *J. Polym. Sci., Part A: Polym. Chem.*, 2016, **54**, 1987–1997.
23 B. M. Alameda, T. C. Palmer, J. D. Sisemore, N. G. Pierini and D. L. Patton, *Polym. Chem.*, 2019, **10**, 5635–5644.
24 M. Pujari-Palmer, H. Guo, D. Wenner, H. Autefage, C. D. Spicer, M. M. Stevens, O. Omar, P. Thomsen, M. Edén, G. Insley, P. Procter and H. Engqvist, *Materials*, 2018, **11**, 2492.
25 Ü. Cural, B. Atalay and M. S. Yildirim, *J. Craniofac. Surg.*, 2018, **29**, 1780–1787.
26 B. Balakrishnan, D. Soman, U. Payanam, A. Laurent, D. Labarre and A. Jayakrishnan, *Acta Biomater.*, 2017, **53**, 343–354.
27 B. Hoffmann, E. Volkmer, A. Kokott, P. Augat, M. Ohnmacht, N. Sedlmayr, M. Schieker, L. Claes, W. Mutschler and G. Ziegler, *J. Mater. Sci. Mater. Med.*, 2009, **20**, 2001–2009.
28 M. Brown, G. W. Kay, D. Cochran, J. Fiorellini and B. Hess, *Society for Biomaterials Annual Meeting and Exposition, 42nd Annual Meeting*, Society for Biomaterials, Mount Laurel, NJ, USA, 2019, vol. 40. From bench-to-bedside: Licensing and development of a mineral-organic bone adhesive for bone repair.169p.
29 A. Kirillova, C. Kelly, N. von Windheim and K. Gall, *Adv. Healthcare Mater.*, 2018, **7**, 1800467.
30 J. d. S. Vieira, F. R. Santos, J. V. de Freitas, F. Baratto-Filho, C. C. Gonzaga and M. R. de Araujo, *Oral Maxillofac. Surg.*, 2016, **20**, 157–160.
31 A. Tzagiollari, H. O. McCarthy, T. J. Levingstone and N. J. Dunne, *Bioengineering*, 2022, **9**, 250.
32 K. J. Schreader, I. S. Bayer, D. J. Milner, E. Loth and I. Jasiuk, *J. Appl. Polym. Sci.*, 2013, **127**, 4974–4982.
33 M. Shokri, F. Dalili, M. Kharaziha, M. Baghaban Eslaminejad and H. Ahmadi Tafti, *Adv. Colloid Interface Sci.*, 2022, **305**, 102706.
34 T. O. Machado, C. Sayer and P. H. H. Araujo, *Eur. Polym. J.*, 2017, **86**, 200–215.
35 L. He, D. Szopinski, Y. Wu, G. A. Luinstra and P. Theato, *ACS Macro Lett.*, 2015, **4**, 673–678.
36 S. C. Ligon, K. Seidler, C. Gorsche, M. Griesser, N. Moszner and R. Liska, *J. Polym. Sci., Part A: Polym. Chem.*, 2016, **54**, 394–406.
37 S. C. Ligon-Auer, M. Schwentenwein, C. Gorsche, J. Stampfl and R. Liska, *Polym. Chem.*, 2016, **7**, 257–286.
38 C. E. Hoyle and C. N. Bowman, *Angew. Chem., Int. Ed.*, 2010, **49**, 1540–1573.
39 S. K. Reddy, N. B. Cramer and C. N. Bowman, *Macromolecules*, 2006, **39**, 3673–3680.
40 C. E. Hoyle and C. N. Bowman, *Angew. Chem., Int. Ed.*, 2010, **49**, 1540–1573.
41 K. Olofsson, V. Granskog, Y. Cai, A. Hult and M. Malkoch, *RSC Adv.*, 2016, **6**, 26398–26405.
42 A. Nordberg, P. Antoni, M. I. Montañez, A. Hult, H. Von Holst and M. Malkoch, *ACS Appl. Mater. Interfaces*, 2010, **2**, 654–657.
43 Y. Hed, K. Öberg, S. Berg, A. Nordberg, H. von Holst and M. Malkoch, *J. Mater. Chem. B*, 2013, **1**, 6015–6019.
44 K. Ganabady, N. Contessi Negrini, J. C. Scherba, B. M. Nitschke, M. R. Alexander, K. H. Vining, M. A. Grunlan, D. J. Mooney and A. D. Celiz, *ACS Appl. Mater. Interfaces*, 2023, **15**, 50908–50915.
45 J. R. Carlise, R. M. Kriegel, W. S. Rees and M. Weck, *J. Org. Chem.*, 2005, **70**, 5550–5560.
46 S.-I. Sasaki, T. Amano, S. Ozawa, T. Masuyama, D. Citterio, H. Hisamoto, H. Hori and K. Suzuki, *J. Chem. Soc., Perkin Trans. 1*, 2001, 1366–1371, DOI: 10.1039/B008978H.
47 B. M. Trost, J. Xu and T. Schmidt, *J. Am. Chem. Soc.*, 2008, **130**, 11852–11853.
48 K. Chougrani, G. Niel, B. Boutevin and G. David, *Beilstein J. Org. Chem.*, 2011, **7**, 364–368.
49 A. Oyane, K. Onuma, A. Ito, H. M. Kim, T. Kokubo and T. Nakamura, *J. Biomed. Mater. Res., Part A*, 2003, **64**, 339–348.
50 P. Steinbauer, A. Rohatschek, O. Andriotis, N. Bouropoulos, R. Liska, P. J. Thurner and S. Baudis, *Langmuir*, 2020, **36**, 13292–13300.
51 N. B. Cramer, S. K. Reddy, A. K. O'Brien and C. N. Bowman, *Macromolecules*, 2003, **36**, 7964–7969.
52 P. Steinbauer, R. Liska and S. Baudis, *Polym. Int.*, 2022, **71**, 790–796.
53 Y. Catel, U. K. Fischer and N. Moszner, *Polym. Int.*, 2013, **62**, 1717–1728.
54 N. Moszner and U. Salz, *Macromol. Mater. Eng.*, 2007, **292**, 245–271.
55 J. C. Todd and E. Braziulis, *Scientific documentation of Adhese universal*, Ivoclar Vivadent AG, 2015.
56 A. Eibel, J. Radebner, M. Haas, D. E. Fast, H. Freissmuth, E. Stadler, P. Faschauner, A. Torvisco, I. Lamparth, N. Moszner, H. Stueger and G. Gescheidt, *Polym. Chem.*, 2018, **9**, 38–47.
57 C. Gorsche, R. Harikrishna, S. Baudis, P. Knaack, B. Husar, J. Laeuger, H. Hoffmann and R. Liska, *Anal. Chem.*, 2017, **89**, 4958–4968.